Evaluation of lattice site and valence of manganese in hexagonal $BaTiO_3$ by electron paramagnetic resonance

2005 J. Phys.: Condens. Matter 17 4925

(http://iopscience.iop.org/0953-8984/17/32/006)

INSTITUTE OF PHYSICS PUBLISHING JOURNAL OF PHYSICS: CONDENSED MATTER

J. Phys.: Condens. Matter **17** (2005) 4925–4934 doi:10.1088/0953-8984/17/32/006

Evaluation of lattice site and valence of manganese in hexagonal $BaTiO_3$ by electron paramagnetic resonance

R Böttcher[1], H T Langhammer[2], T Müller[3] and H-P Abicht[3]

[1] Fakultät für Physik und Geowissenschaften, Universität Leipzig, Linnéstraße 5, 04103 Leipzig, Germany
[2] Fachbereich Physik, Martin-Luther-Universität Halle Wittenberg, Friedemann-Bach-Platz 6, 06108 Halle, Germany
[3] Fachbereich Chemie, Martin Luther-Universität Halle-Wittenberg, Kurt-Mothes-Straße 2, 06120 Halle, Germany

E-mail: boettch@physik.uni-leipzig.de

Received 25 May 2005, in final form 6 July 2005
Published 29 July 2005
Online at stacks.iop.org/JPhysCM/17/4925

Abstract

The electron paramagnetic resonance (EPR) spectra of $BaTi_{1-x}Mn_xO_3$ ceramics powder ($0.005 \leqslant x \leqslant 0.016$) were studied in different frequency bands (9 and 34 GHz). In as-sintered and air-annealed samples two different, axially symmetric EPR spectra assigned to Mn^{4+} ions are observed. The manganese impurities are substituted at Ti sites corresponding to the different distorted octahedra in the 3C and 6H modification of $BaTiO_3$. The temperature dependence of these EPR spectra allowed the unambiguous assignment of the paramagnetic ions to the lattice site in cubic and hexagonal modification. After annealing the samples in reducing atmosphere a drastic change in the EPR spectra is observed. Only isolated Mn^{2+} ions and associates consisting of Mn^{2+} ions and oxygen vacancies in the 3C modification of $BaTiO_3$ are detected.

1. Introduction

The hexagonal polymorph of 6H-$BaTiO_3$ (h-$BaTiO_3$) crystallizes in the space group $P6_3/mmc$ with the lattice parameters $a = 0.5738$ nm and $c = 1.3965$ nm [1, 2]. The unit cell is described by six BaO_3 layers (i.e. $[Ba(2)O(2)_3Ba(2)O(2)_3Ba(1)O(1)_3]_2$) forming a $(cch)_2$ sequence, where c corresponds to corner-sharing and h to face-sharing layers of the TiO_6 octahedra, respectively (for labelling the atoms see [1]). The atoms Ti(1) and Ti(2) occupy octahedra which are exclusively corner-connected and which are sharing common faces, respectively, with rather short Ti(2)–Ti(2) distances in the Ti_2O_9 groups consisting of two face-sharing octahedra. In contrast to cubic 3C-$BaTiO_3$ the octahedra in h-$BaTiO_3$ are trigonally distorted

in the *c*-direction. The strength of the distortion in the corner- and face-sharing octahedra is different. Therefore, in the hexagonal modification there are two different Ti lattice sites. Four of six Ti-ions in each hexagonal unit cell are incorporated into the face-sharing octahedra whereas the other two are lying in the exclusively corner-sharing ones.

Glaister and Kay [3] first reported in 1960 that certain amounts of Mn are sufficient to stabilize the hexagonal phase of $BaTiO_3$ at room temperature whereas the hexagonal polymorph of undoped material is stable in air only at temperatures higher than 1703 K [4]. Two possibilities are known to stabilize h-$BaTiO_3$ at lower temperatures. The first one is firing in reducing atmospheres (oxygen-deficient $BaTiO_3$). In pure hydrogen a temperature of 1603 K is sufficient for the transformation into the hexagonal phase. Recently, Sinlcair *et al* [5] determined the crystal structure of a series of oxygen-deficient $BaTi^{4+}_{1-x}Ti^{3+}_{x}O_{3-x/2}$ ($0 < x < 0.30$). In this material the hexagonal perovskite structure is retained throughout and partial reduction of Ti^{4+} to Ti^{3+} is accompanied by the formation of only O(1) oxygen vacancies. Changes in cell unit dimensions are dominated by an increase in Ti(2)–Ti(2) separation within face-sharing octahedra. Doping with 3d transition elements, like Cr, Mn, Fe, Ni or Cu, is the second way of stabilizing h-$BaTiO_3$ at room temperature [3, 6–8]. Grey *et al* [9] reported on x-ray diffraction (XRD) investigations of h-$BaMO_{3-d}$ (M = Ti, Fe) material where Ti^{4+} was progressively replaced by Fe^{3+} and/or Fe^{4+} with oxygen vacancies being formed exclusively in O(1) sites within the h-BaO_3 layers. Removal of O(1) results in an increased repulsion between M(2) atoms within the face-sharing octahedra and hence in a lengthening of the M(2)–M(2) distance.

The question, at which Ti lattice site and with which states of valence the paramagnetic ions M are incorporated into the h-$BaTiO_3$ is an open problem. For this purpose we performed EPR investigations on Mn-doped $BaTiO_3$ at a doping level of between 0.5 and 1.6 mol%. EPR spectroscopy is an excellent tool for identifying transition metal dopants which are frequently introduced into $BaTiO_3$ in order to modify the crystal structure, conductivity and grain boundary properties [10–13]. It is able to yield valuable information on the oxidation state of the paramagnetic ion, the local symmetry of its lattice site and the strength of the electrical field. Furthermore, EPR measurements allow us to determine the degree of the association of oxygen vacancies with paramagnetic defects [14].

2. Experimental procedure

Ceramic powder with a nominal composition of $BaTi_{1-x}Mn_xO_3$ ($0.005 \leqslant x \leqslant 0.016$) was prepared by the conventional mixed-oxide powder technique. The samples were sintered in air at $T_s = 1673$ K for 1 h. Then, portions of the samples were annealed in air and in a gas stream of a mixture of Ar and H_2 (1:1), respectively, and were characterized with respect to their microstructure and phase composition. In both cases the annealing was accomplished at 1473 K for 2 h. All heat treatments took place with heating and cooling rates of 10 K min^{-1}. Further details of the preparation and characterization as well as the results are given in [6].

EPR measurements of the pulverized samples were carried out in the X-band with a Varian E112 spectrometer and in the Q-band with a Bruker EMX device. For the evaluation of the powder EPR spectra and the determination of the spin-Hamiltonian parameters the MATLAB[4] toolbox for electron paramagnetic resonance 'Easy Spin 2.0.3' was used [15]. By simultaneously simulating the X- and Q-band spectra by variation of the input parameters, a high accuracy in the determination of the spectra parameters was achieved.

[4] MATLAB is a registered trademark of the MathWorks, Inc., Natick, MA, USA.

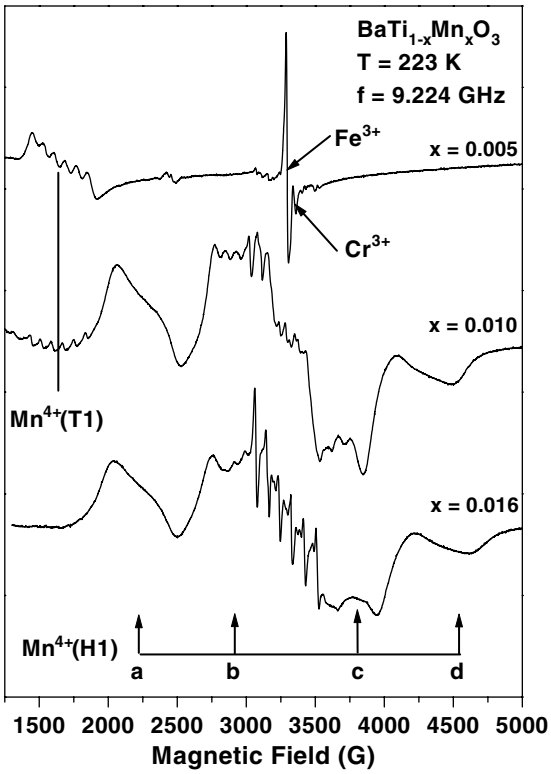

Figure 1. X-band EPR spectrum of $BaTi_{1-x}Mn_xO_3$ samples with different concentration x (0.005, 0.010, 0.016). The samples were annealed in air at 1473 K and their spectra recorded at 223 K.

3. Results

3.1. As-sintered and air-annealed samples

Figure 1 shows the EPR spectra measured at 223 K of as-sintered $BaTi_{1-x}Mn_xO_3$ with $x = 0.005$, 0.010 and 0.016. In the case of $x = 0.005$ the spectrum is identical with that of $BaTiO_3$ reported by several workers [11, 16, 17] and consists of two sets of hyperfine groups with six lines: one set at $g_{\text{eff}} \approx 4.35$ (labelled by T1) and the other with very small intensity in the region $g \approx 2.00$. Of the most interest is the line sextet at $g_{\text{eff}} = 4.35$. In a crystalline field of axial symmetry, the spin Hamiltonian of a paramagnetic ion with $S = 3/2$ or $5/2$ may be written as

$$\widehat{H} = g_{\parallel}\beta\,\widehat{S}_z B_z + g_{\perp}\beta(\widehat{S}_x B_x + \widehat{S}_y B_y) + D(\widehat{S}_z^2 - \tfrac{1}{3}S(S+1)) + A_{\parallel}\widehat{S}_z\widehat{I}_z + A_{\perp}(\widehat{S}_x\widehat{I}_x + \widehat{S}_y\widehat{I}_y). \quad (1)$$

Here, the various terms have their normal spectroscopic meaning [18]. Structural variations in the immediate surroundings of the paramagnetic ions cause variations in the fine structure (fs) parameters. The fs parameter distributions are assumed to be random, so they can be approximated by symmetric Gaussian distributions with the full width at half height ΔD and ΔE, respectively. For $S = 5/2$ (Mn^{2+}) fourth-order terms in the S-operators have to be added to (1).

In the case of the strong axial crystalline field ($|D| \gg g\beta B$) the fine structure energy is the dominant term in the spin Hamiltonian and the observed EPR spectrum may be explained by

the effective electron spin $S_{\mathrm{eff}} = 1/2$ with the effective, strongly angular-dependent g-factor g_{eff} [19]

$$g_{\mathrm{eff}}(\theta) = [g_{\parallel}^2 + (m^2 g_{\perp}^2 - g_{\parallel}^2)\sin^2\theta]^{\frac{1}{2}} \left[1 - \frac{n^2}{4}\frac{(g_{\perp}\beta B)^2}{(2D)^2}F(\theta)\right],$$

where

$$F(\theta) = \sin^2\theta \left[\frac{(m^2 g_{\perp} + 2g_{\parallel})\sin^2\theta - 2g_{\parallel}}{(m^2 g_{\perp} - g_{\parallel})\sin^2\theta + g_{\perp}}\right], \tag{2}$$

$m = 2$, $n = \sqrt{3}$ and $m = 3$, $n = 2\sqrt{2}$ for $S = 3/2$ and $S = 5/2$, respectively. $g_{\parallel}$ and $g_{\perp}$ are the principal values of the axial g-tensor of the true spin Hamiltonian (1). The sextet with $g_{\mathrm{eff}} = 4.35$ is a typical transition between the $|\pm 1/2\rangle$ doublet of a spin-3/2 ion in a strong axial field. The spin-Hamiltonian parameters determined from X- and Q-band measurements are in agreement with the results given in [16]. Thus an unambiguous assignment of this spectrum to Mn^{4+} ions ($S = 3/2$, $I = 5/2$) substituted at Ti^{4+} lattice sites in the 3C-polytype of $BaTiO_3$ is given. The other hyperfine group of the six very weak lines in the range $g \approx 2.000$ is interpreted as the central transition $M_S = 1/2 \leftrightarrow M_S = -1/2$ of a Mn^{2+} ($S = 5/2$, $I = 5/2$) spectrum. In addition in the field range of 3300 G intensive lines are detected which are generated by paramagnetic impurities (Fe^{3+} and Cr^{3+}) in the raw materials.

On going to higher Mn concentration ($x = 0.01$), the powder spectrum changes drastically and a new partial spectrum (labelled by H1) with poorly-resolved peaks appears (see figure 1). Four fine structure transitions labelled by a, b, c, and d are observed in the range from 1500 to 5000 G of the X-band spectrum. Out of this range there are two further peaks with very weak intensities. Only the peaks b and c show a hyperfine splitting, which is well visible in the Q-band spectrum (figure 2). With growing manganese concentration x, the intensity of H1 spectrum is increased; in contrast, the intensity of the sextet with $g \approx 4.35$ decreases. In the case of $x = 0.016$ it is no longer detectable, and additionally to the H1 spectrum a six-line spectrum is observed in the magnetic-field range corresponding to $g \approx 2.00$. The positions of the peaks a–d, which are broadened by dipole–dipole interaction, variation of the fine structure parameters and hyperfine interaction of the unpaired electrons with the nuclear magnetic moment of ^{55}Mn (nuclear spin $I = 5/2$), have a strong temperature dependence (figure 3). Below $T = 218$ K an additional splitting of all peaks of the H1 spectrum is measured, but this is hardly to be seen in figure 3 due to the weak peak intensities.

The comparison of the X- and Q-band spectra of the as-sintered $BaTiO_{1-x}Mn_xO_3$ samples as well as the study of their temperature dependence allowed the disentanglement of the powder spectra. The details of the powder spectra for paramagnetic centres with $S = 3/2$ are given in [20]. The observed peaks a, b, c, and d are allowed fine structure transitions $\Delta M_S = \pm 1$ of one $S = 3/2$ spin system, which may also described at room temperature by an axially symmetric spin Hamiltonian (1) and the assignment of the peaks is the following: a and b belong to the transitions $M_S = \pm 3/2 \leftrightarrow M_S = \pm 1/2$, $\theta = \pi/2$, c to the central transition $M_S = -1/2 \leftrightarrow M_S = +1/2$, $\theta = \pi/2$ and the peak d to $M_S = -1/2 \leftrightarrow M_S = 1/2$, $\theta = 0.2322\pi$. θ is the angle between the symmetry axis of the fine structure interaction tensor and the external magnetic field. The peaks with $M_S = \pm 3/2 \leftrightarrow M_S = \pm 1/2$, $\theta = 0$ lie out of the scan range of the spectrum (figure 1). Simultaneous simulation of the X- and Q-band powder spectra permitted the unambiguous determination of the electron spin ($S = 3/2$) of the paramagnetic ions as well as the evaluation of the temperature-dependent spin-Hamiltonian parameters. Below 218 K this spectrum has to be explained by a spin Hamiltonian of rhombic symmetry. The results are given in tables 1 and 2. Figure 2 shows the satisfying coincidence between the experimental and simulated Q-band spectrum H1 of a sample with $x = 0.016$.

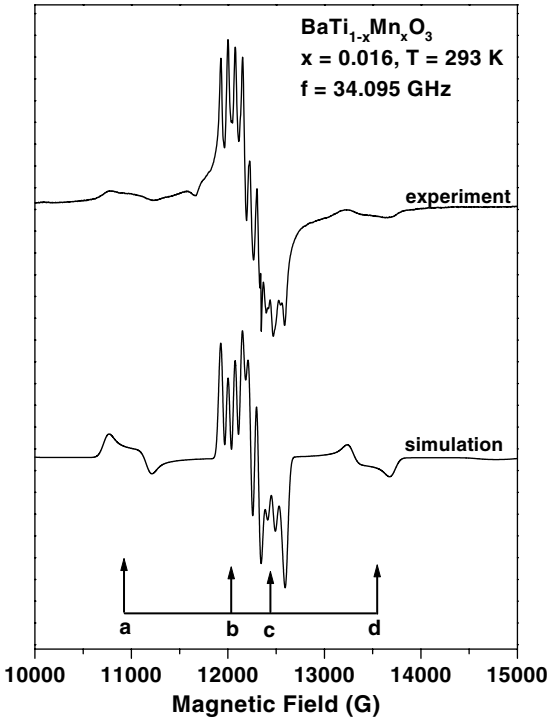

Figure 2. Experimental and simulated Q-band spectrum H1 of $BaTi_{1-x}Mn_xO_3$ samples with $x = 0.016$. For the simulation the spin Hamiltonian (1) and the parameters given in table 1 were used.

Table 1. Room-temperature spin-Hamiltonian parameters of the $Mn^{4+}_{Ti(1)}$ (H1) centre in the 6H modification of $BaTi_{1-x}Mn_xO_3$ ($x = 0.01$). For comparison the values of the Mn^{4+}_{Ti} (T1) ion incorporated into the 3C modification (rhombohedral low-temperature phase) are given [11]. The hfs and fs parameters, their dispersions and their errors are given in 10^{-4} cm^{-1}.

Centre	$g_\parallel$	$g_\perp$	$\lvert D\rvert$	ΔD	$\lvert A_\parallel\rvert$	$\lvert A_\perp\rvert$
$Mn^{4+}_{Ti(1)}$ (H1)	1.9901(8)	1.9932(8)	1160(30)	150(20)	60(2)	68(2)
Mn^{4+}_{Ti} (T1)	2.0015(5)	1.9968(19)	6500(500)	—	44.3(5)	72.9(3)

Table 2. Temperature dependence of the fs parameters of the $Mn^{4+}_{Ti(1)}$ (H1) centre in the 6H modification of $BaTi_{1-x}Mn_xO_3$ ($x = 0.01$). The values are given in 10^{-4} cm^{-1}.

T (K)	$\lvert D\rvert$	$\lvert E\rvert$	ΔD	ΔE
523	1600(30)	—	150(20)	—
473	1500(30)	—	150(20)	—
273	1160(30)	—	130(20)	—
223	970(30)	—	120(20)	—
173	940(30)	40(20)	120(20)	20(20)

In the air-annealed samples the same partial EPR spectra are observed; however, their relative intensities are changed in comparison to the as-sintered samples.

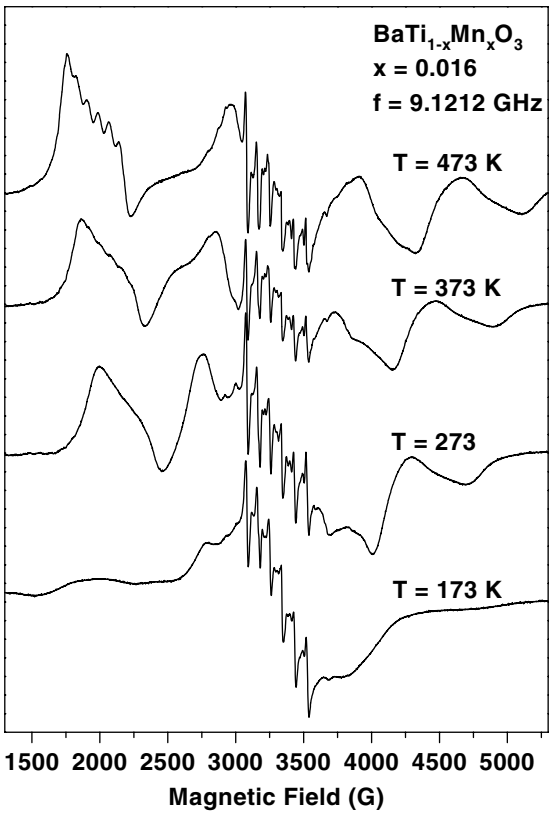

Figure 3. Temperature dependence of the X-band spectrum of $BaTi_{1-x}Mn_xO_3$ samples with $x = 0.016$. The well-resolved sextet with $g \approx 2.00$ is assigned to Mn^{2+} ions. Below $T = 220$ K the peaks of the H1 spectrum reveal a splitting due to symmetry reduction.

3.2. Samples annealed in reducing atmosphere

The powder spectra of $BaTi_{1-x}Mn_xO_3$ ($x = 0.005$, 0.010 and 0.016) annealed in reducing atmosphere are shown in figure 4; they differ considerably from those of the as-sintered and air-annealed samples. The shape of the spectra is almost independent of the Mn concentration x. Each powder spectrum may be decomposed into two partial spectra: one spectrum at $g \approx 2.00$ and the other one in the region $g_{\text{eff}} \approx 6.00$. The partial spectrum with $g \approx 2.00$ consists of several fine structure peaks due to the electron spin $S = 5/2$. Only the central peak with $M_S = -1/2 \leftrightarrow M_S = 1/2$ is well resolved whereas the others are broadened by dipole–dipole interaction and D-strain effects. In contrast to the H1 spectrum this partial one reveals temperature dependence. A significant change is observed in the vicinity of the phase transitions of the 3C modification of $BaTiO_3$, in particular, at the transition from the rhombohedral to orthorhombic and from the tetragonal to the cubic phase, respectively. The alteration can be attributed to changes of the local symmetry and the parameters of the spin Hamiltonian (with $S = 5/2$ and $I = 5/2$, determined by multi-frequency EPR investigations) rather than changes in the oxidation state of the manganese ion. The evaluated spin-Hamiltonian parameters are in agreement with the results presented in [16] and therefore are not given here. In accordance with the discussion in [16], it may be concluded that this

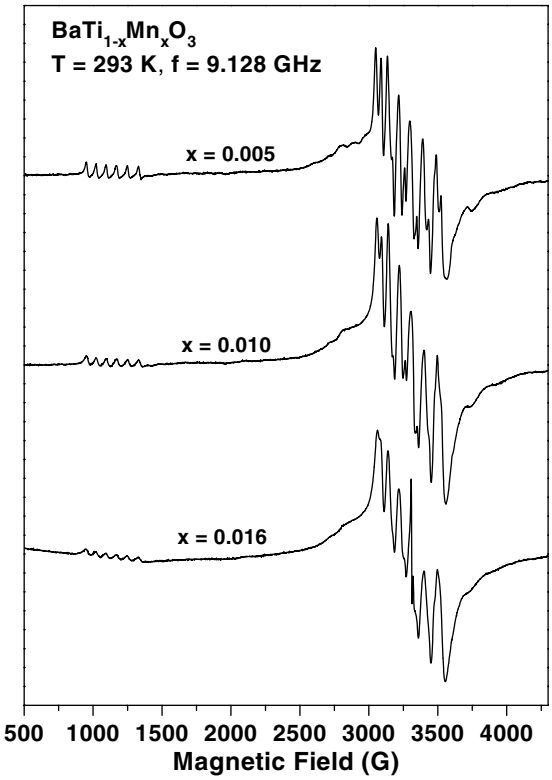

Figure 4. X-band EPR spectrum of $BaTi_{1-x}Mn_xO_3$ samples with different concentrations x (0.005, 0.010, 0.016). All samples were annealed in reducing atmosphere. The spectra were recorded at 293 K.

partial spectrum has to be assigned to isolated Mn^{2+} ions ($S = 5/2$) which are incorporated at Ti^{4+} lattice sites in the 3C modification.

In contrast to the partial spectrum with $g \approx 2.00$, the other partial spectrum only consists of one sextet with $g_{\text{eff}} = 6.00$ in the X-band. On going to higher frequencies (Q-band), more peaks with hyperfine splitting were detectable, which can be classified by the axially symmetric spin Hamiltonian (1) with the electron spin $S = 5/2$. The multi-line Q-band EPR spectrum permits the conclusion that this manganese spectrum can also be explained by an axial fs parameter D which is of the same order of magnitude as the X-band Zeeman energy. The spectral parameters determined by simultaneous simulation of the X- and Q-band spectra with the pepper function of the MATLAB (see footnote 4) toolbox for electron paramagnetic resonance 'Easy Spin 2.0.3' [15] are also given in table 3. Surprisingly, its spin-Hamiltonian parameters are almost temperature independent, and no further additional splitting is observed on varying the temperature from 173 to 423 K.

4. Discussion

Manganese can substitute Ti in the 3C and 6H modification of $BaTiO_3$ exhibiting oxidation states of 4+ (electron configuration d^3, ground state ^4F with $S = 3/2$), 3+ (d^4, ^5D with $S = 2$) and 2+ (d^5, ^6A with $S = 5/2$). Because of the weak spin–lattice interaction of the

Table 3. Room-temperature spin-Hamiltonian parameters of the Mn_{Ti}^{2+}–V_O centre in the 3C modification of $BaTi_{1-x}Mn_xO_3$ ($x = 0.016$, reduced samples) determined by Q-band measurements. The hfs and fs parameters, their dispersions and their errors are given in 10^{-4} cm^{-1}. The principal values of the g-tensors have an accuracy of ±0.0008.

Centre	$g_\parallel$	$g_\perp$	$\lvert D\rvert$	ΔD	$\lvert A_\parallel\rvert$	$\lvert A_\perp\rvert$
Mn_{Ti}^{2+}–V_O	2.0002	2.0002	3750(30)	40(10)	75(2)	75(2)

non-degenerated orbital ground state in the electrical crystalline field of octahedral symmetry, only the oxidation states of the isolated manganese impurity 4+ and 2+ are detectable with EPR spectroscopy in the temperature range above 73 K.

In as-sintered and air-annealed $BaTi_{1-x}Mn_xO_3$ samples with $x = 0.005$ the manganese has the valence state Mn^{4+} or Mn^{3+}, and only a minor part is in the divalent state. In the case of Mn^{3+} and Mn^{2+}, the electroneutrality is maintained by the formation of oxygen vacancies. The concentration of the Jahn–Teller-active Mn^{3+} ions is too low to induce the transformation from the cubic to the hexagonal modification [6]. In agreement with the XRD measurement (cp figure 1 in [6]) at room temperature, the ceramic material is in the tetragonal phase of the 3C polytype. On going to higher x-values, the concentration of both Mn^{4+} and Mn^{3+} ions is increased. Owing to the non-uniform distribution of the manganese ions in the $BaTiO_3$ grains there are grains in which the local Mn^{3+} concentration is higher than the critical one. In these grains the transmutation to the hexagonal modification take place and a new $S = 3/2$ EPR spectrum, the Mn^{4+}-H1 spectrum, appears. In contrast to the tetragonal crystal structure of the 3C polytype, the oxygen octahedra in the h-$BaTiO_3$ unit cell are trigonally distorted along the hexagonal c-axis. The strength of the trigonal distortion for the corner- (with the Ti(1) site) and face-sharing (with the Ti(2) site) octahedra is different. Therefore, in the 6H modification there are two crystallographically different Ti lattice sites. If there tetravalent manganese ions are incorporated on both Ti(1) and Ti(2) sites, the occurrence of two different powder spectra with unequal spin-Hamiltonian parameters is expected. However, only the H1 spectrum is observed in $BaTi_{1-x}Mn_xO_3$ with $x \geqslant 0.010$. We assign it to Mn^{4+} ions on the Ti(1) lattice sites in the exclusively corner-sharing octahedra $Ti(1)O(2)_6$ in which the Ti(1)–O(2) distances are equal. Due to the hexagonal structure at room temperature the local symmetry of the Ti(1) site is reduced to the trigonal one by the presence of the next-nearest neighbours. In comparison with the Ti(2) site, the electrical field, which is responsible for the fine structure splitting, is weaker at the Ti(1) site. Because the dopant Mn^{4+} has the same charge as the replaced Ti^{4+} ion, charge compensation is not necessary. Oxygen vacancies and other impurities are not present in the immediate surroundings of Mn^{4+} ions and no further distortion of the octahedron is expected. For this reason the H1 spectrum reflects the local symmetry of the undisturbed Ti(1) lattice site not only at room temperature but also at low temperature. Consequently, the symmetry of the spin Hamiltonian describing the H1 spectrum is related to the crystal symmetry which is changed at the phase transitions of the lattice with 6H stacking [21]:

hexagonal–orthorhombic–monoclinic

220 K 74 K.

In contrast with chromium-doped h-$BaTiO_3$, in which the EPR spectrum of Cr^{3+} ions substituted on Ti(2) site was also detected [20], this spectrum was not observed in $BaTi_{1-x}Mn_xO_3$ ($0 < x < 0.05$). One can speculate that only the Mn^{3+} ions occupy the Ti(2) site in the face-sharing octahedra because the oxygen vacancies necessary for the electroneutrality were produced by removal of O(1) atoms in the Ti_2O_9 groups [8].

The sextet at $g \approx 2.00$ detected in the sample with $x = 0.016$ has the typical values of a Mn^{2+} spin Hamiltonian. We assign these hfs peaks to the central transition $M_S = -1/2 \leftrightarrow M_S = 1/2$ to a small amount of isolated Mn^{2+} ions in the 6H modification. An in-depth investigation of this centre was not performed.

A completely changed EPR powder spectrum, almost independent of the manganese concentration x, was measured in the samples annealed in reducing atmosphere. By this heat treatment of the material the oxygen is readily exchanged between the solid and the surrounding atmosphere according to the reaction

$$O_O^{2-} = V_O + 2e^- + \tfrac{1}{2}O_2\uparrow. \tag{3}$$

The electrons produced by reaction (3) are associated with the oxygen vacancies but can either be thermally activated to free carriers even at room temperature due to the vicinity of these levels to the conduction band edge or change the valence state of existing acceptor-type ions, leading in our case to the presence of Mn^{3+} and Mn^{2+}. Due to the strong reduction condition in our experiment the majority of manganese is probably in the 2+ valence state. Hence, the driving force of the transformation cubic → hexagonal, the Jahn–Teller distortion of the Mn^{3+} ion [6], is now missing. Otherwise, the temperature of the reducing treatment of 1473 K is well below the cubic–hexagonal transformation temperature in undoped material. Thus, the samples with $x = 0.010$ and 0.016 are completely re-transformed into the 3C polytype, which was also proved by XRD [6].

In the powder EPR spectrum only Mn^{2+} ions are detected. One of the partial Mn^{2+} spectra which reflects all phase transitions of the 3C modification is assigned to isolated divalent manganese ions. The second centre observed in reduced samples of $BaTi_{1-x}Mn_xO_3$ ($0 < x < 0.05$) gives rise to a highly anisotropic transition ($S_{\text{eff}} = 1/2$) with hyperfine splitting having peaks in the powder spectrum at $g_\perp^{\text{eff}} = 6.00$ and $g_\parallel^{\text{eff}} = 2.00$ (not visible in the X-band spectrum due to the overlapping with the other intensive Mn^{2+} spectrum). Since the parameters a and F of the fourth-order S-terms which appear in the spin Hamiltonian of Mn^{2+} ions are usually very small compared to D, only the axial crystal field D is evaluated by simulation of both X- and Q-band spectra to be 0.375 cm^{-1}. This is about an order of magnitude larger than the fs parameter observed for isolated Mn^{2+} ions in the tetragonal phase of the cubic modification [16, 17]. Very large axial fields have been reported for the Fe^{3+} ion in $BaTiO_3$, $SrTiO_3$ and other perovskites which arise from a nearest-neighbour oxygen vacancy (Fe^{3+}–V_O) [14, 22, 23]. In analogy to these defect association centres, we assign this axial manganese spectrum to the Mn^{2+}–V_O centre. Because the Mn^{2+} ion substitutes Ti^{4+} and O^{2-} is lacking, the Mn^{2+}–V_O defect is neutrally charged with respect to the lattice. The spectrum of the Mn^{2+}–V_O associate ($D \approx 0.544$ cm^{-1}) in an Mn-doped single crystal of $SrTiO_3$ was investigated by Serway *et al* [22].

5. Conclusions

Manganese-doped barium titanate ceramics consist of parts of 3C- and 6H-stacked crystallites depending on the doping level. Manganese is incorporated at Ti sites in both crystallographic surroundings, and is reflected in well-distinguishable EPR spectra. Whereas the EPR spectra of the 3C-stacked crystallites (as-sintered samples) exhibit the well-known behaviour (major defect Mn_{Ti}^{4+} with hfs sextet at $g = 4.35$, minor defect Mn_{Ti}^{2+} with hfs sextet at $g = 2.00$), hexagonal Mn-doped $BaTiO_3$ shows the H1 EPR spectrum of Mn_{Ti}^{4+} ($S = 3/2$) with four fs peaks around $g = 2.00$. The analysis of the spectrum in the X- and Q-band shows that Mn_{Ti}^{4+} is incorporated only at Ti(1) sites of the hexagonal lattice (exclusively corner-sharing octahedra).

Samples which were annealed under heavily reducing conditions are completely retransformed into the 3C modification. Their X-band spectra consist of two partial spectra at $g_{\text{eff}} = 6.00$ and $g = 2.00$ which are caused by Mn^{2+}_{Ti}. The lines near $g = 2.00$ are attributed to isolated Mn^{2+}_{Ti} centres whereas the others are caused by neutral Mn^{2+}_{Ti}–V_O associates.

Acknowledgments

The authors thank Professor Dr D Michel for helpful discussions and Mrs U Heinich and Dipl.-Ing. J Hoentsch for the measurements of the EPR spectra. These investigations were financially supported by the Deutsche Forschungsgemeinschaft (DFG-Schwerpunktprogramm 'Hochfeld-EPR in Biologie, Chemie and Physik', SPP 1051).

References

[1] Burbank R D and Evans H T Jr 1948 *Acta Crystallogr.* **1** 330
[2] Akimoto J, Gotoh Y and Oosawa Y 1994 *Acta Crystallogr.* C **50** 160
[3] Glaister R M and Kay H F 1960 *Proc. Phys. Soc.* **76** 763
[4] Kirby K W and Wechsler B A 1991 *J. Am. Ceram. Soc.* **74** 1841
[5] Sinclair D C, Skakke J M S, Morrison F D, Smith R I and Beales T P 1999 *J. Mater. Chem.* **9** 1327
[6] Langhammer H L, Müller T, Felgner K-H and Abicht H-P 2000 *J. Am. Ceram. Soc.* **83** 605
[7] Langhammer H T, Müller T, Böttcher R and Abicht H-P 2003 *Solid State Sci.* **5** 965
[8] Keith G M, Rampling M J, Sarma K, Mc Alford N and Sinclair D C 2004 *J. Eur. Ceram. Soc.* **24** 1721
[9] Grey J E, Li Ch, Cranswick L M D, Roth R S and Vanderah T A 1988 *J. Solid State Chem.* **135** 312
[10] Müller K A, Berlinger W and Albers J 1985 *Phys. Rev.* B **32** 5837
[11] Müller K A 1991 *Structural Phase Transitions II* ed K A Müller and H Thomas (Berlin: Springer)
[12] Possenriede E, Schirmer O F, Albers J and Godefroy G 1990 *Ferroelectrics* **107** 313
[13] Scharfschwerdt R, Mazur A, Schirmer O F, Hesse H and Mendricks S 1996 *Phys. Rev.* **54** 15284
[14] Merkle R and Maier J 2003 *Phys. Chem. Chem. Phys.* **5** 2297
[15] Stoll St 2003 Spectral simulations in solid-state EPR *PhD Thesis* ETH Zurich
[16] Milsch B 1992 *Phys. Status Solidi* a **133** 455
[17] Schwartz R and Wechsler B 1993 *Phys. Rev.* B **48** 7057
[18] Weil J A, Wertz J E and Bolton J R 1994 *Electron Spin Resonance: Elementary Theory and Practical Applications* (New York: Wiley)
[19] Kirkpatrick E S, Müller K A and Rubins R S 1964 *Phys. Rev.* **135** 86A
[20] Böttcher R, Erdem E, Langhammer H T, Müller T and Abicht H-P 2005 *J. Phys.: Condens. Matter* **17** 2763
[21] Sawaguchi E, Akishige Y and Kobayashi M 1985 *J. Phys. Soc. Japan* **54** 480
[22] Serway R A, Berlinger W, Müller K A and Collins R W 1977 *Phys. Rev.* **16** 4761
[23] Müller K A 1981 *J. Physique* **36** 551